The solar wind's geomagnetic impact and its Sun–Earth evolution

Predictive models for space weather and for the Parker Solar Probe orbit

PhD defense by
Malte Venzmer

PhD student
within the doctoral program ProPhys,
Georg-August University School of Science
(GAUSS)

Institute for Astrophysics
Georg-August-Universität Göttingen

Examination board members
Dr. Volker Bothmer (supervisor, referee)
Prof. Dr. Ansgar Reiners (2nd referee)
Prof. Dr. Stefan Dreizler
Prof. Dr. Wolfram Kollatschny
Prof. Dr. Hardi Peter
Prof. Dr. Andreas Tilgner

Thursday, 1 November 2018, 14:00
Seminarraum Astrophysik (SR 17, F 05.104)

Contents

Contents

The solar wind's geomagnetic impact and its Sun–Earth evolution
Predictive models for space weather and for the Parker Solar Probe orbit

Geomagnetic impact of the solar wind

Solar wind – solar system bodies
CMEs – geomagnetic storms – effects
Importance of prediction of onset/magnitude
The study addresses; deriving predictive models

Geomagnetic impact of the solar wind

- Kp index
- Coupling mechanisms
- Reconnection at magnetopause

Geomagnetic impact of the solar wind

Relations between the Kp index and solar wind parameters:

Electric field proxy (vB_z)

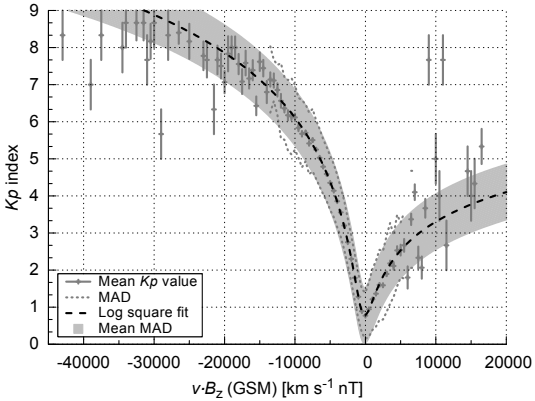

Velocity of CMEs and streams

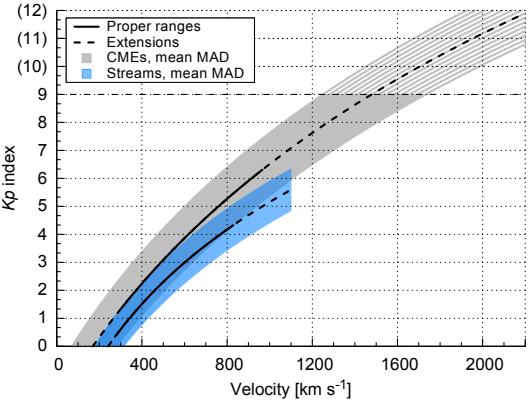

Solar wind

- E. Parker's theoretical model
- Confirmation by in-situ measurements
- Monitored continuously near Earth since

Solar wind

- E. Parker's theoretical model
- Confirmation by in-situ measurements
- Monitored continuously near Earth since

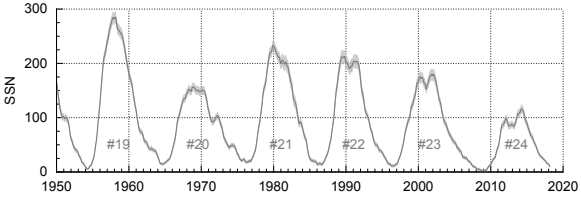

Solar wind

- E. Parker's theoretical model
- Confirmation by in-situ measurements
- Monitored continuously near Earth since

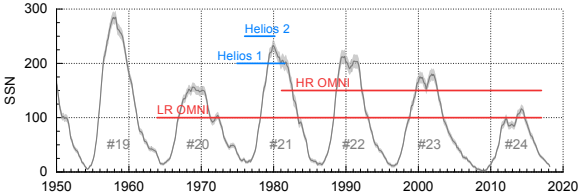

Measured in-situ throughout the heliosphere:

- Voyager – heliopause
- Ulysses – high heliolatitudes
- Helios – Mercury

Solar wind

Credit: Miloslav Druckmüller, Zuzana Druckmüllerová, Jana Hoderová, Peter Štarha, Shadia Habbal, 2017

The near-Sun region is of special scientific interest:

- Coronal heating
- Solar wind acceleration

Parker Solar Probe

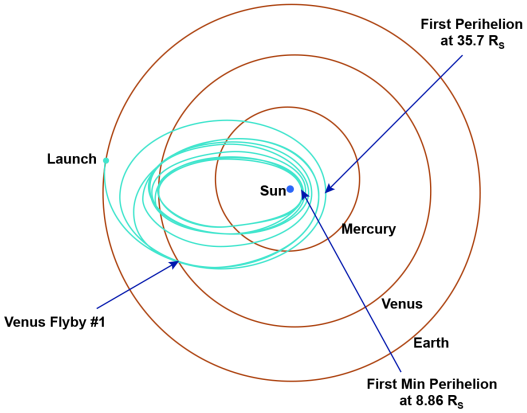

Credit: NASA/Johns Hopkins APL, 2018

Parker Solar Probe

Credit: NASA/Johns Hopkins APL/Ed Whitman, 2018

Parker Solar Probe

Credit: NASA/Johns Hopkins APL/Ed Whitman, 2018

12 August 2018: launched
3 October: Venus flyby
29 October: closest s/c ever (63.5 $R_\odot$)
6 November: first perihelion (36.7 $R_\odot$)
24 December 2024: first closest perihelion (9.86 $R_\odot$)

PSP mission goals (Fox et al., 2015)

- Trace flow of energy that heats and accelerates the corona and solar wind
- Determine the structure and dynamics of the plasma and magnetic fields at the sources of the solar wind
- Explore the mechanisms that accelerate and trannsport solar energetic particles

WISPR coronagraph (Wide-Field Imager for Solar Probe)
This study is based on work performed for the CGAUSS (Coronagraphic German and US SolarProbePlus Survey) project

Solar wind model

Aim
use existing solar wind data
empirical solar wind model
extrapolate model to PSP orbit

Solar wind model

Model concept

Solar wind key parameters

- Magnetic field strength
- Velocity
- Density
- Temperature

values shifted according to solar activity and solar distance
unique: frequency distributions

PSP distance and SSN prediction

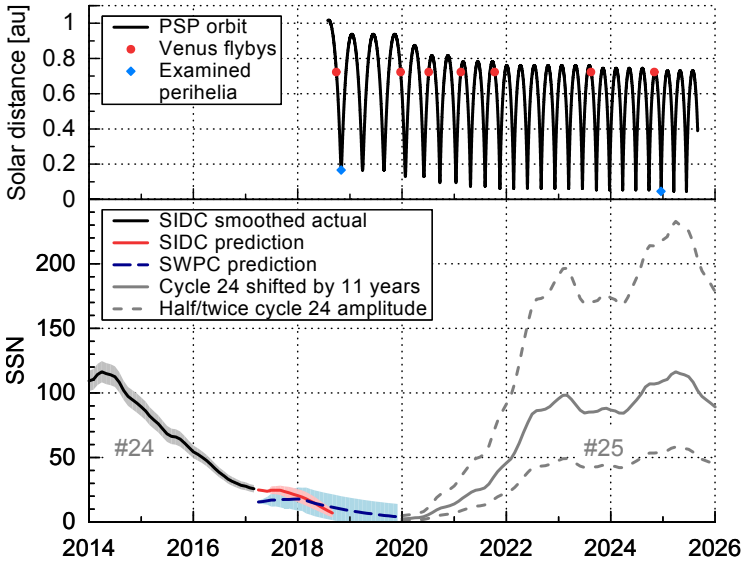

PSP distance and SSN prediction

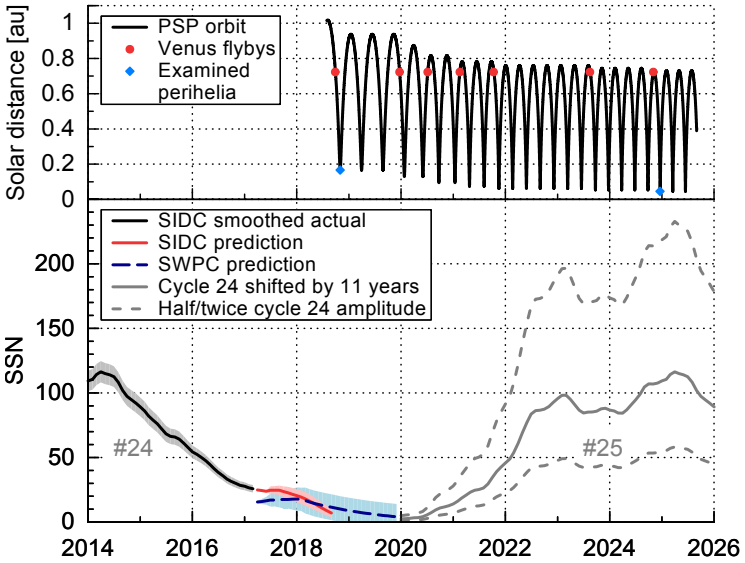

2018: solar minimum
2024: solar maximum

OMNI data set

OMNI data set (King & Papitashvili, 2005)
- intercalibrated multi-spacecraft data
- time-shifted to the bow shock of the magnetosphere
- 1963–2016

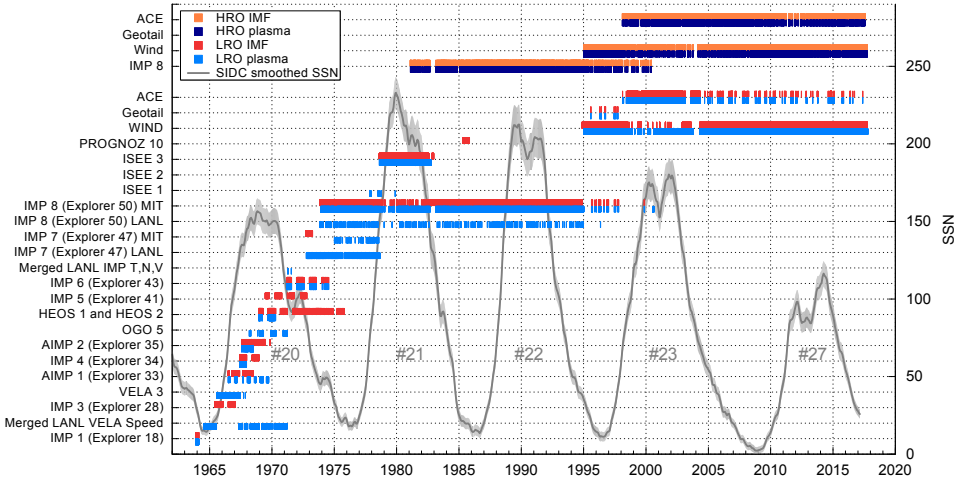

OMNI data set

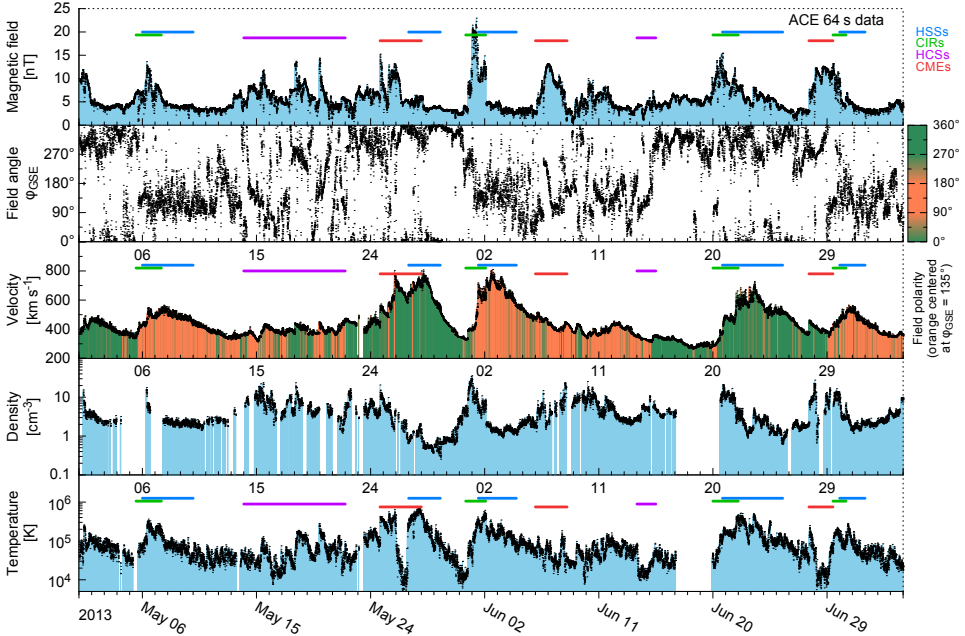

Frequency distributions

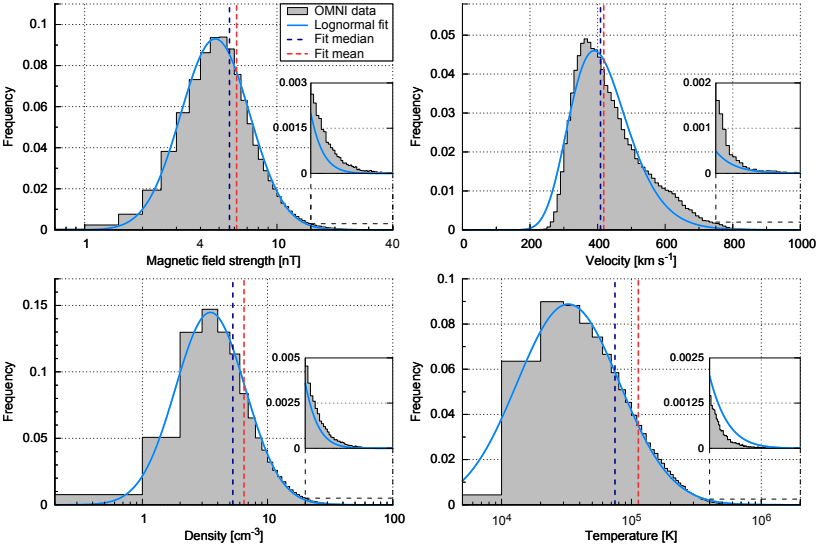

Lognormal distribution

Frequency distributions

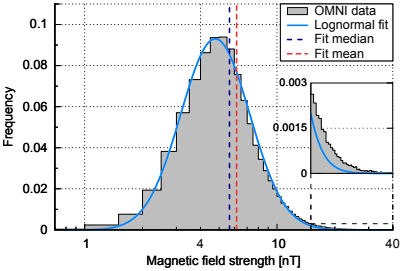

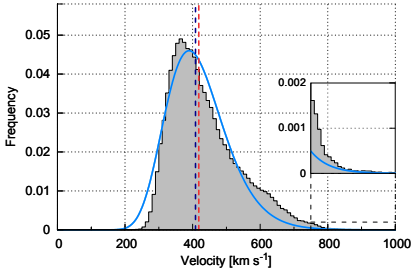

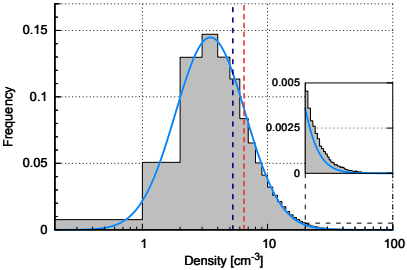

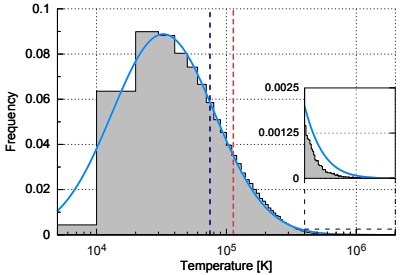

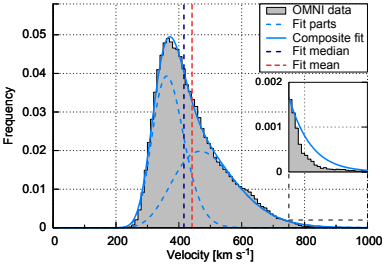

Lognormal distribution

Solar activity

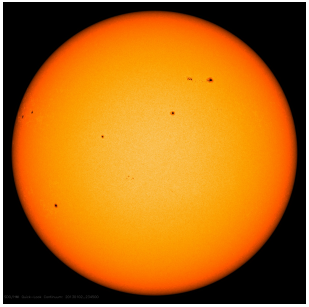

Credit: NASA SDO/HMI, 1 January 2013

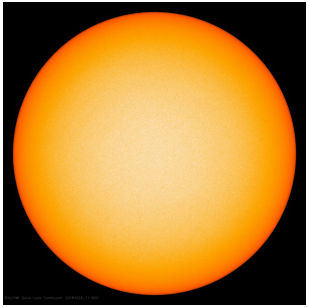

Credit: NASA SDO/HMI, 26 October 2018

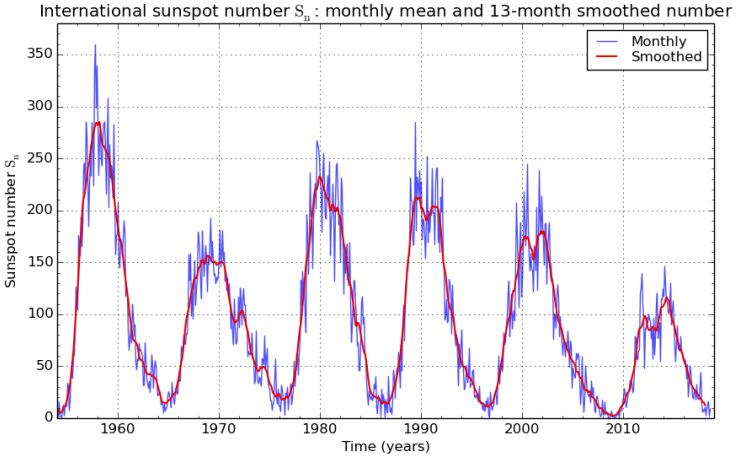

SILSO graphics (http://sidc.be/silso) Royal Observatory of Belgium 2018 September 1

⏩ Magnetic butterfly diagram

Solar activity

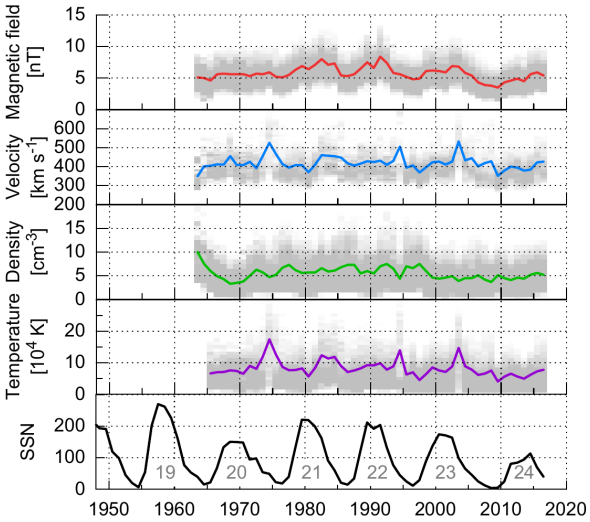

Solar activity

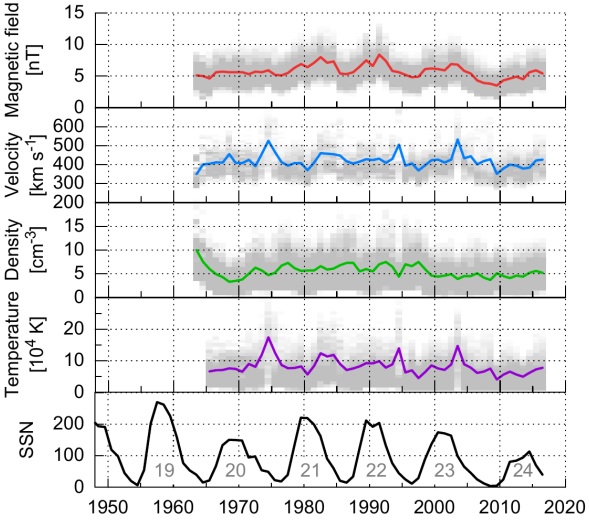

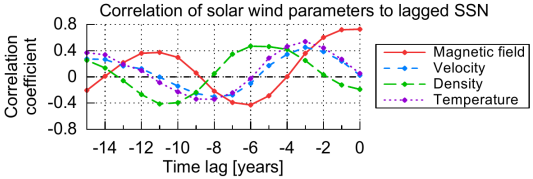

Solar activity

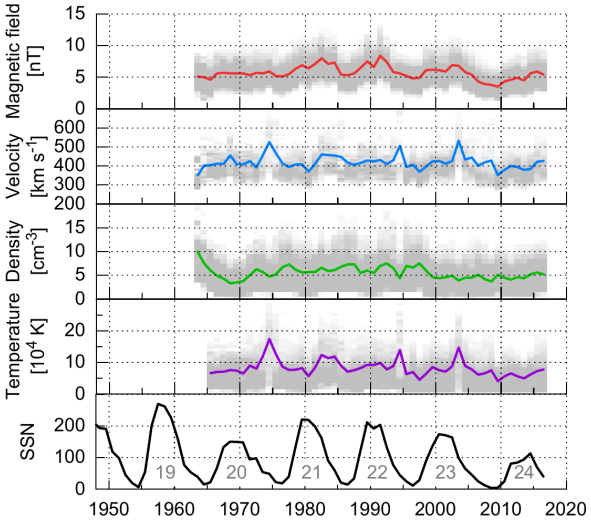

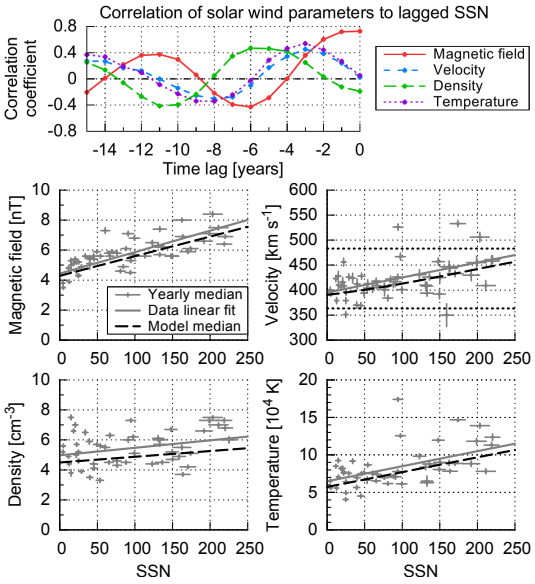

Solar activity

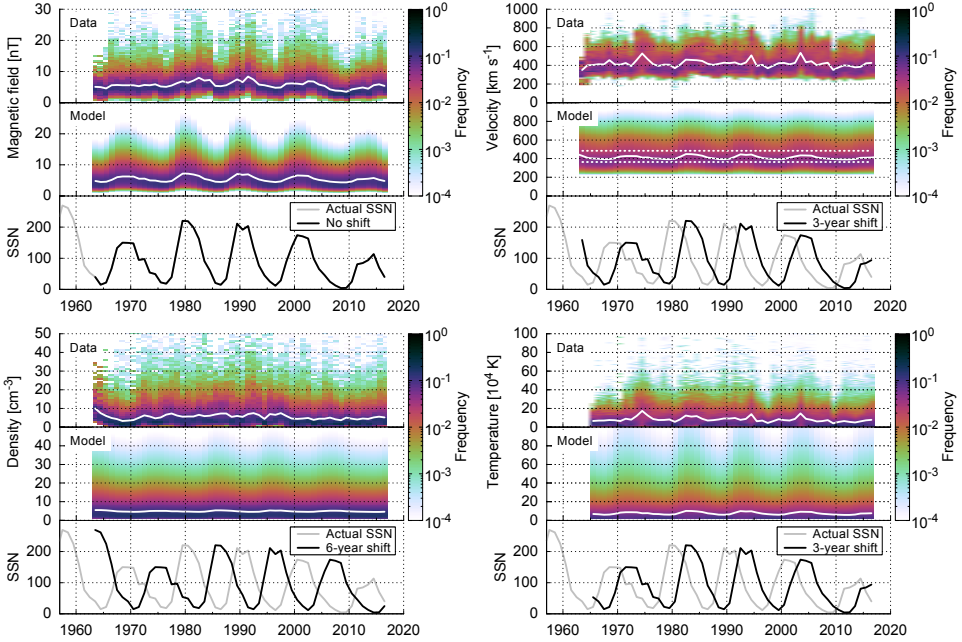

Helios data

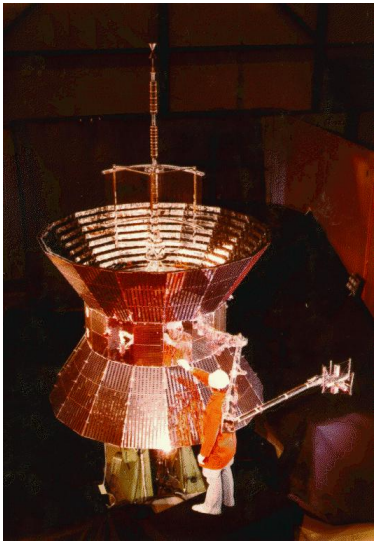

Credit: NASA

Helios 1 and Helios 2
hourly data set (Rosenbauer et al., 1977)
0.29–0.98 au
1974–1981

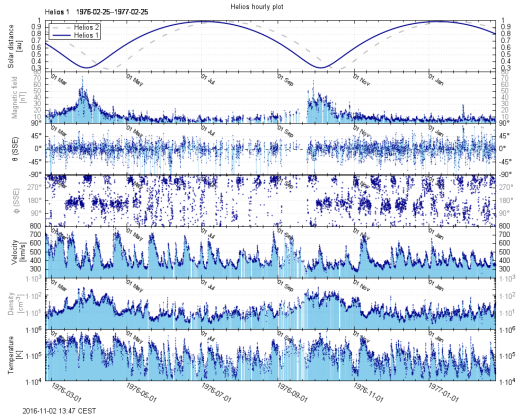

Solar distance

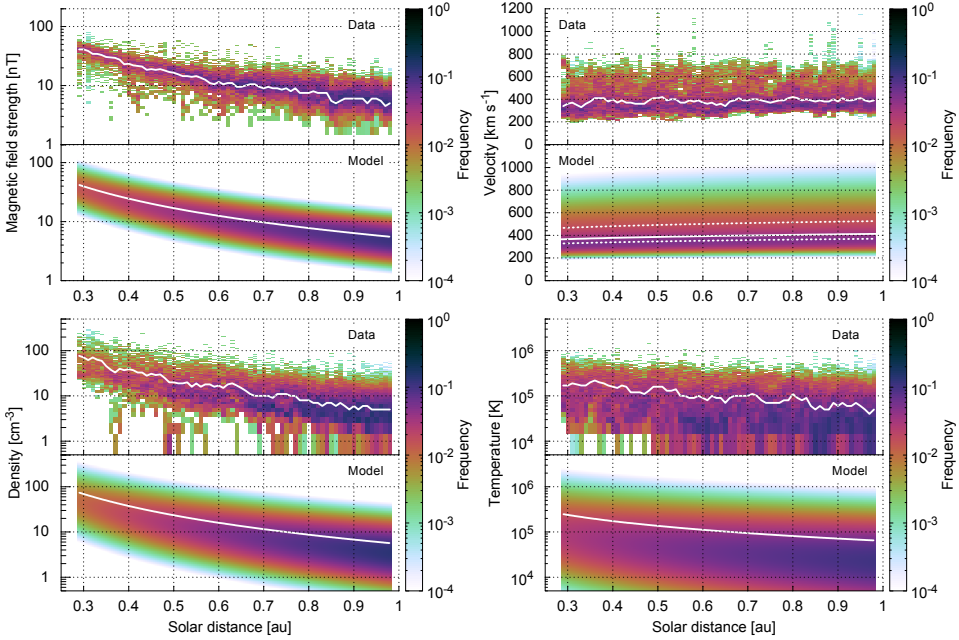

PSP's current position

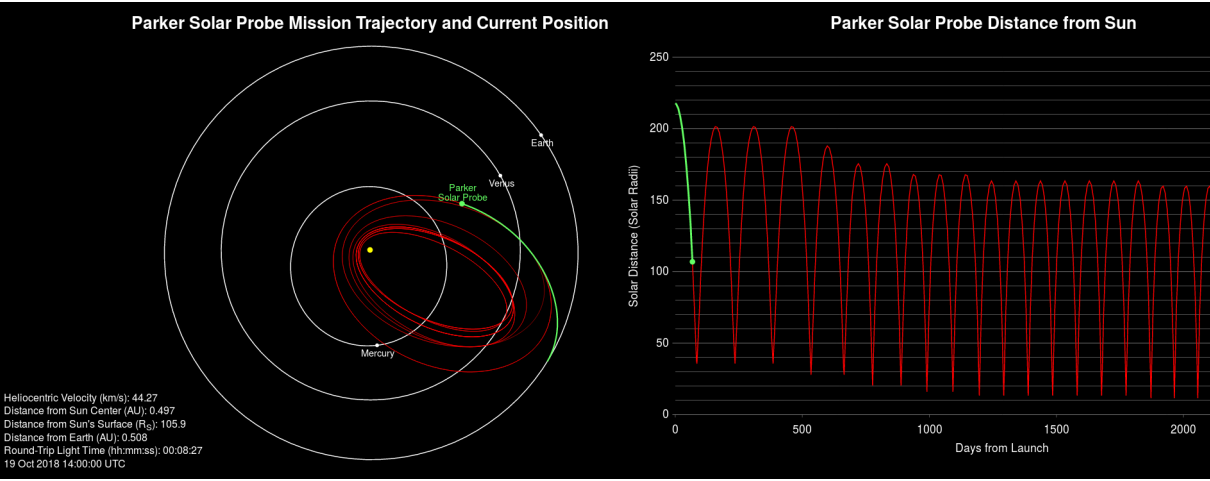

Credit: NASA

Prediction for PSP orbit

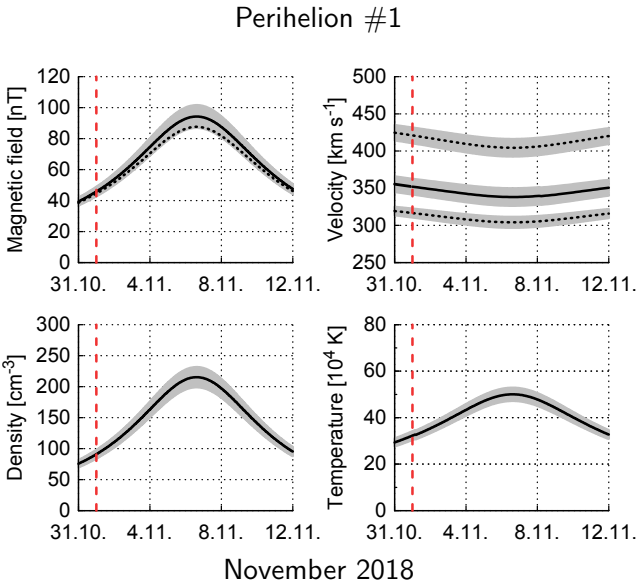

Prediction for PSP orbit

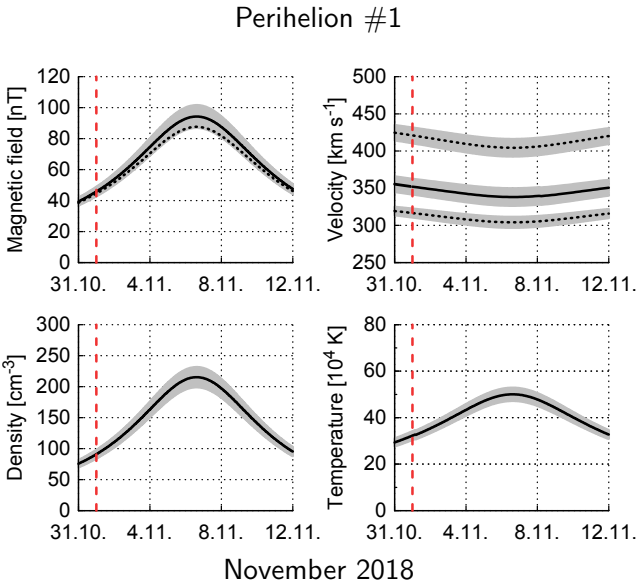

Predicted values at 36.7 $R_\odot$

$B = 94\,\mathrm{nT}$

$v = 340\,\mathrm{km\,s^{-1}}$

$n = 214\,\mathrm{cm^{-3}}$

$T = 5.03 \times 10^5\,\mathrm{K}$

Prediction for PSP orbit

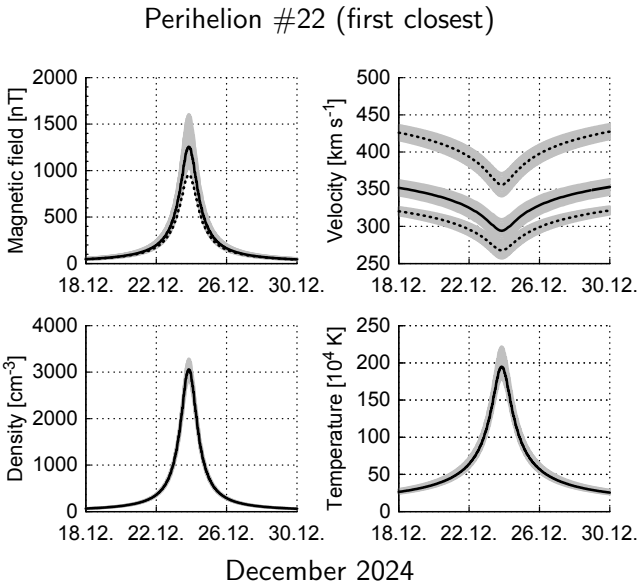

Prediction for PSP orbit

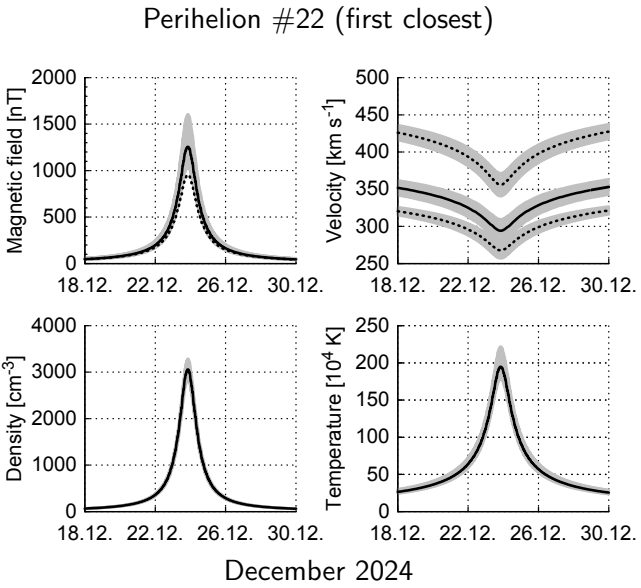

Predicted values at 9.86 $R_\odot$

$B = 1241\,\mathrm{nT}$

$v = 290\,\mathrm{km\,s^{-1}}$

$n = 2951\,\mathrm{cm^{-3}}$

$T = 1.93 \times 10^6\,\mathrm{K}$

Predicted values at 9.86 $R_\odot$

$$B = 1241\,\mathrm{nT}$$
$$v = 290\,\mathrm{km\,s^{-1}}$$
$$n = 2951\,\mathrm{cm^{-3}}$$
$$T = 1.93 \times 10^6\,\mathrm{K}$$

Predicted values at 9.86 $R_\odot$

$$B = 1241\,\mathrm{nT}$$
$$v = 290\,\mathrm{km\,s^{-1}}$$
$$n = 2951\,\mathrm{cm^{-3}}$$
$$T = 1.93 \times 10^6\,\mathrm{K}$$

Remote observations show the limits of the model:

- Studies reveal slow wind velocities of $200\,\mathrm{km\,s^{-1}}$ (Sheeley et al., 1997; Wang et al., 2000)
- Near-Sun coronal temperatures yield 2–3 MK (Billings, 1959; Liebenberg et al., 1975)

Predicted values at 9.86 $R_\odot$

$$B = 1241\,\mathrm{nT}$$
$$v = 290\,\mathrm{km\,s^{-1}}$$
$$n = 2951\,\mathrm{cm^{-3}}$$
$$T = 1.93 \times 10^6\,\mathrm{K}$$

Remote observations show the limits of the model:

- Studies reveal slow wind velocities of 200 $\mathrm{km\,s^{-1}}$ (Sheeley et al., 1997; Wang et al., 2000)
- Near-Sun coronal temperatures yield 2–3 MK (Billings, 1959; Liebenberg et al., 1975)

$\Rightarrow$ Solar wind is still being heated and accelerated up to 20 $R_\odot$

Outlook

- Investigate near-Sun properties of inner solar wind structures
- Modifications to model
- Refine model with additional solar wind data
  - from Mercury probes
  - from Solar Orbiter
  - from Parker Solar Probe

Summary

- Predictive models that relate geomagnetic disturbances with specific solar wind parameters:
  - Solar wind electric field
  - CME velocity
  - Stream velocity
- Empirical solar wind model for the inner heliosphere that considers solar activity and solar distance
  - Extrapolation of the model to the near-Sun environment for the PSP orbit
  - Solar wind prediction for PSP's first and first closest perihelia

References I

Billings, D. E. 1959, *Distribution of Matter with Temperature in the Emission Corona.*, Astrophys. J., 130, 961, [DOI], [ADS].

Bothmer, V. & Schwenn, R. 1998, *The structure and origin of magnetic clouds in the solar wind*, Annales Geophysicae, 16, 1, [DOI], [ADS].

Cranmer, S. R. & van Ballegooijen, A. A. 2005, *On the Generation, Propagation, and Reflection of Alfvén Waves from the Solar Photosphere to the Distant Heliosphere*, Astrophys. J., Suppl. Ser., 156, 265, [DOI], [ADS].

Davies, K. 1990, *Ionospheric Radio* (Institution of Engineering and Technology), [link], [DOI].

Fox, N. J., Velli, M. C., Bale, S. D. et al. 2015, *The Solar Probe Plus Mission: Humanity's First Visit to Our Star*, Space Sci. Rev., [DOI], [ADS].

Hathaway, D. H. 2015, *The Solar Cycle*, Living Reviews in Solar Physics, 12, 4, [DOI], [ADS].

Hughes, W. J. 1995, *Chapter 9: The magnetopause, magnetotail, and magnetic reconnection*, ed. M. Kivelson & C. Russell, Introduction to Space Physics (Cambridge University Press, Cambridge), 227–287, [ADS].

Liebenberg, D. H., Bessey, R. J. & Watson, B. 1975, *Coronal emission line profile observations at total solar eclipses. II - 30 May 1965 results, deconvolution and interpretation*, Solar Phys., 44, 345, [DOI], [ADS].

King, J. H. & Papitashvili, N. E. 2005, *Solar wind spatial scales in and comparisons of hourly Wind and ACE plasma and magnetic field data*, Journal of Geophysical Research (Space Physics), 110, 2104, [DOI], [ADS].

Marubashi, K. & Lepping, R. P. 2007, *Long-duration magnetic clouds: a comparison of analyses using torus- and cylinder-shaped flux rope models*, Annales Geophysicae, 25, 2453, [DOI], [ADS].

McComas, D. J., Ebert, R. W., Elliott, H. A. et al. 2008a, *Weaker solar wind from the polar coronal holes and the whole Sun*, Geophys. Res. Lett., 35, L18103, [DOI], [ADS].

Owens, M. J. & Forsyth, R. J. 2013, *The Heliospheric Magnetic Field*, Living Reviews in Solar Physics, 10, 5, [DOI], [ADS].

Parker, E. N. 1958, *Dynamics of the Interplanetary Gas and Magnetic Fields.*, Astrophys. J., 128, 664, [DOI], [ADS].

Pizzo, V. J. 1991, *The evolution of corotating stream fronts near the ecliptic plane in the inner solar system. II - Three-dimensional tilted-dipole fronts*, J. Geophys. Res., 96, 5405, [DOI], [ADS].

Rosenbauer, H., Schwenn, R., Marsch, E. et al. 1977, *A survey on initial results of the HELIOS plasma experiment*, Journal of Geophysics Zeitschrift Geophysik, 42, 561, [ADS].

Schatten, K. H., Wilcox, J. M. & Ness, N. F. 1969, *A model of interplanetary and coronal magnetic fields*, Solar Phys., 6, 442, [DOI], [ADS].

Sheeley, N. R., Wang, Y.-M., Hawley, S. H., et al. 1997, Astrophys. J., 484, 472

Venzmer, M. S. & Bothmer, V. 2018, *Solar-wind predictions for the Parker Solar Probe orbit. Near-Sun extrapolations derived from an empirical solar-wind model based on Helios and OMNI observations*, Astron. Astrophys., 611, A36, [DOI], [ADS].

Wang, Y.-M., Sheeley, N. R., Socker, D. G., Howard, R. A. & Rich, N. B. 2000, *The dynamical nature of coronal streamers*, J. Geophys. Res., 105, 25133, [DOI], [ADS].

Thank you!

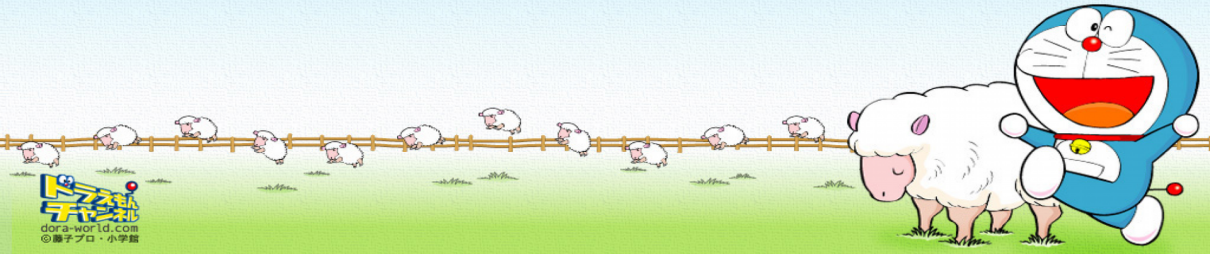

Solar activity
Magnetic butterfly diagram

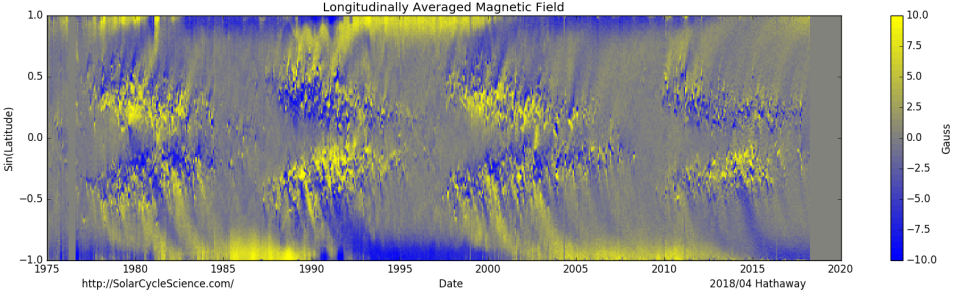

Courtesy of David Hathaway, Solar Cycle Science, 2018, updated version of Hathaway (2015, Fig. 17)

Solar wind

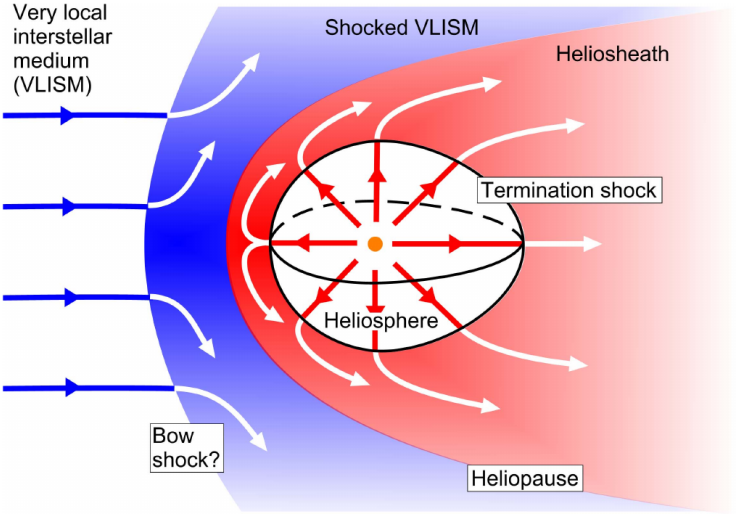

Credit: Owens & Forsyth (2013, Fig. 9)

Solar wind

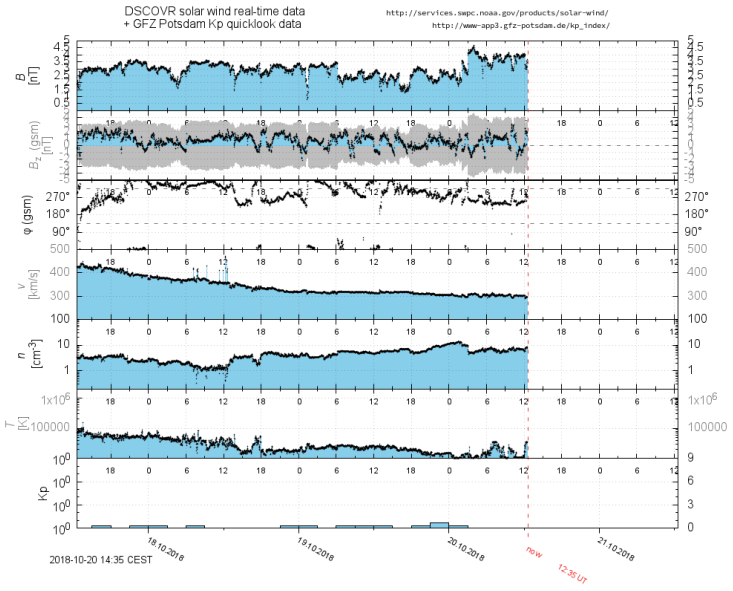
DSCOVR solar wind real-time data
+ GFZ Potsdam Kp quicklook data
http://services.swpc.noaa.gov/products/solar-wind/
http://www-app3.gfz-potsdam.de/kp_index/
B [nT]
B_z (gsm) [nT]
φ (gsm)
v [km/s]
n [cm^{-3}]
T [K]
Kp
2018-10-20 14:35 CEST
18.10.2018
19.10.2018
20.10.2018
21.10.2018
now 12:35 UT

Solar magnetic field

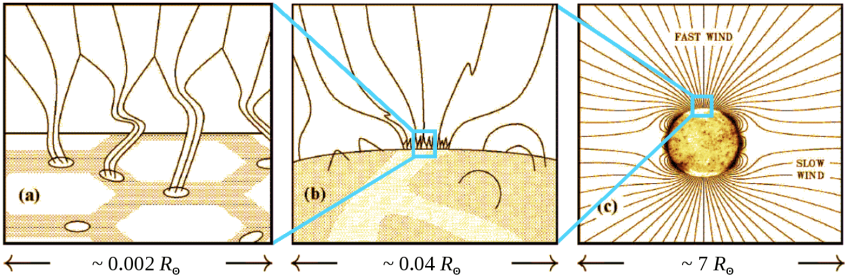

Courtesy of S. R. Cranmer

Solar magnetic field

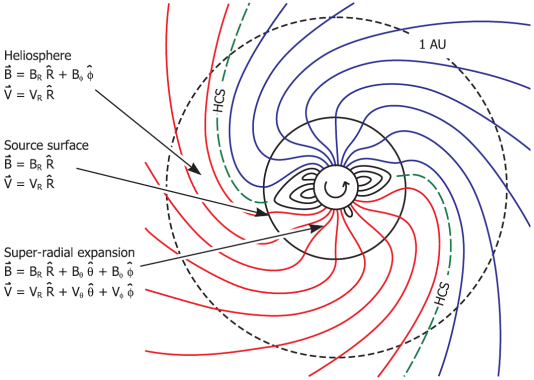

Credit: Owens & Forsyth (2013, Fig. 1), adapted from Schatten et al. (1969, Fig. 1)

Slow and fast solar wind

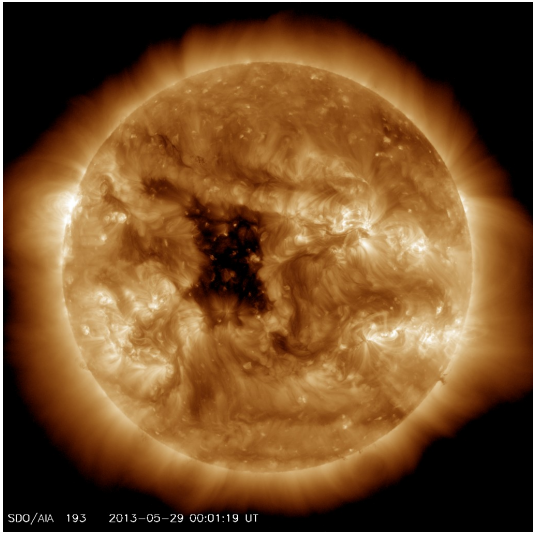

Credit: NASA/SDO and the AIA, EVE and HMI science teams

Slow and fast solar wind

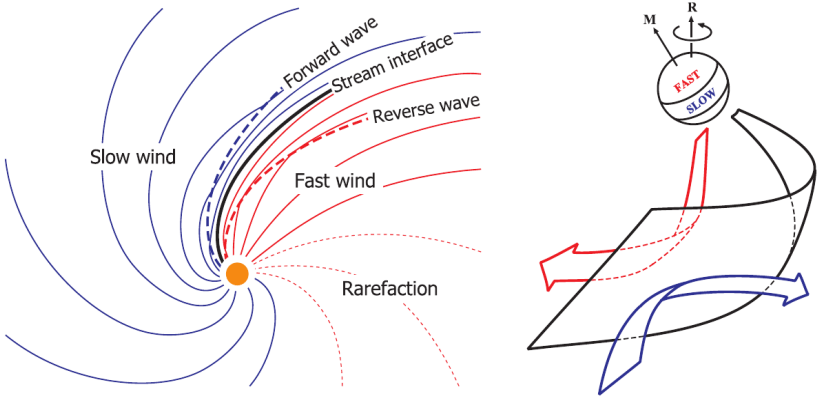

Credit: Owens & Forsyth (2013, Fig. 7); right panel adapted from Pizzo (1991, Fig. 2)

Solar activity

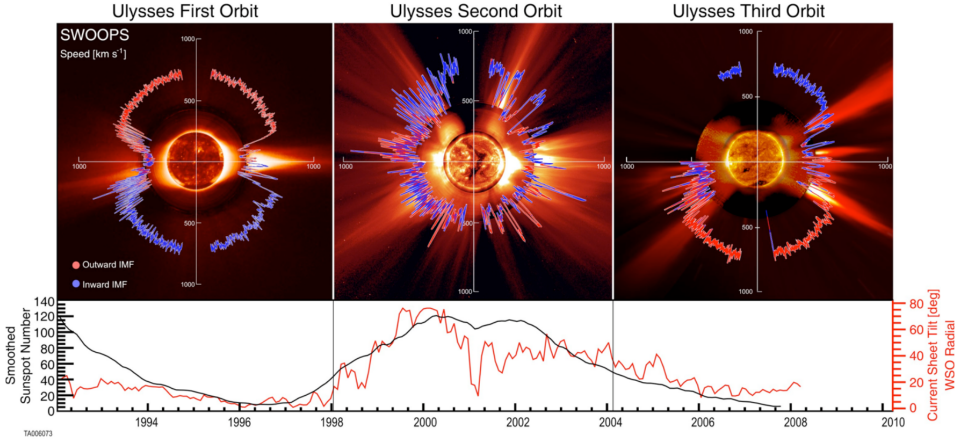

Credit: McComas et al. (2008a, Fig. 1)

Coronal mass ejections

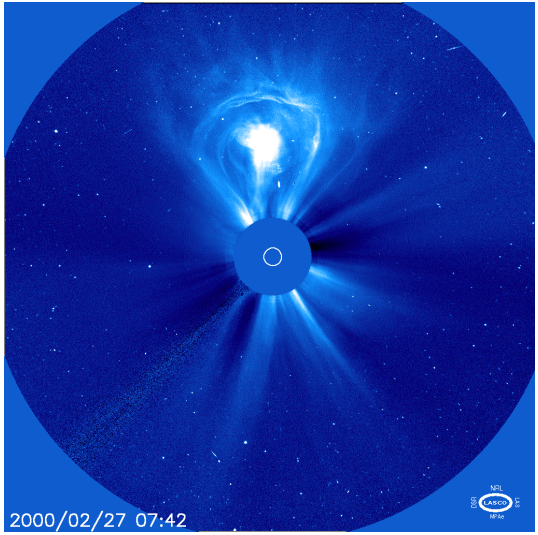

Courtesy of SOHO/LASCO consortium. SOHO is a project of international cooperation between ESA and NASA

Coronal mass ejections

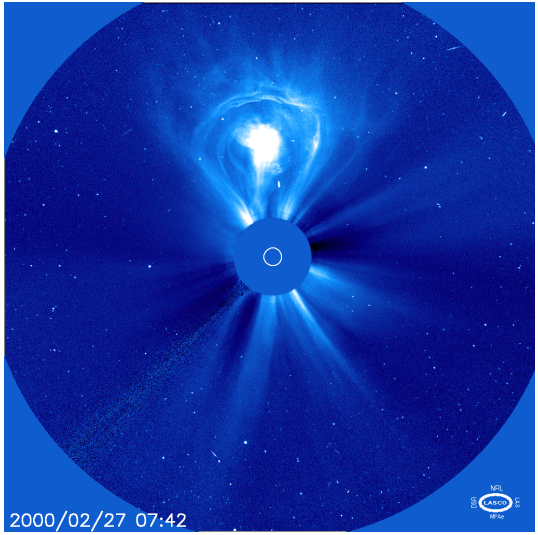

Courtesy of SOHO/LASCO consortium. SOHO is a project of international cooperation between ESA and NASA

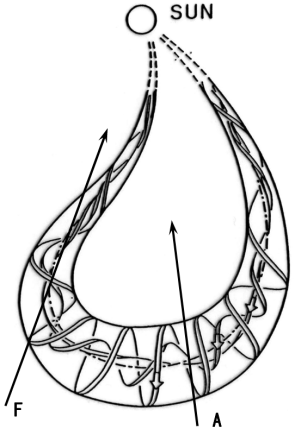

Credit: Marubashi & Lepping (2007, Fig. 1, panel (a))

Coronal mass ejections

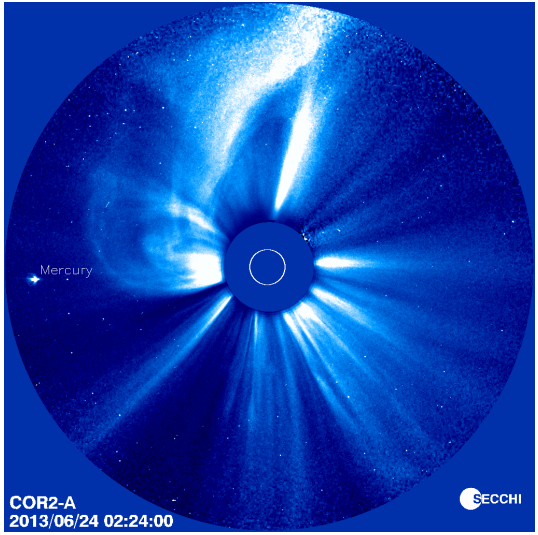

Courtesy of STEREO/COR2 consortium (NASA)

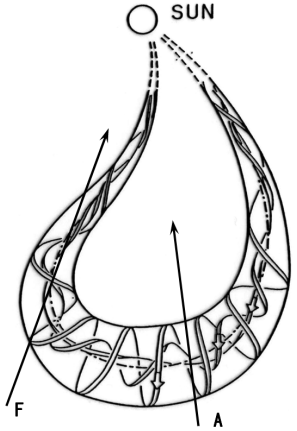

Credit: Marubashi & Lepping (2007, Fig. 1, panel (a))

Coronal mass ejections

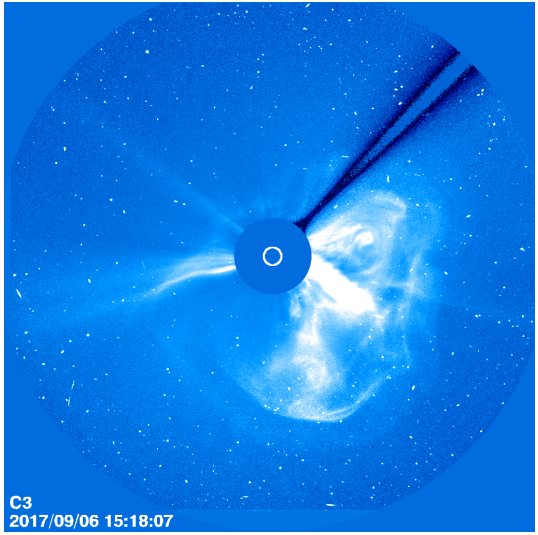

Courtesy of SOHO/LASCO consortium; SOHO is a project of international cooperation between ESA and NASA

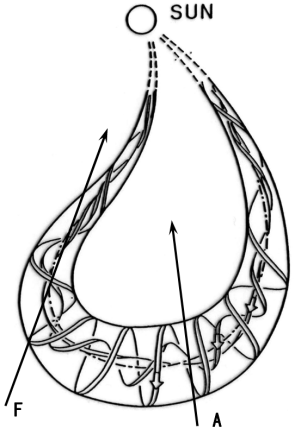

Credit: Marubashi & Lepping (2007, Fig. 1, panel (a))

CME orientation

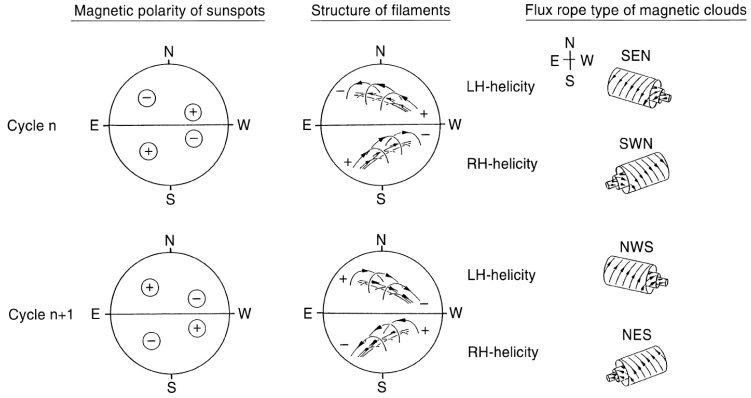

Credit: Bothmer & Schwenn (1998, Fig. 18)

In-situ CMEs

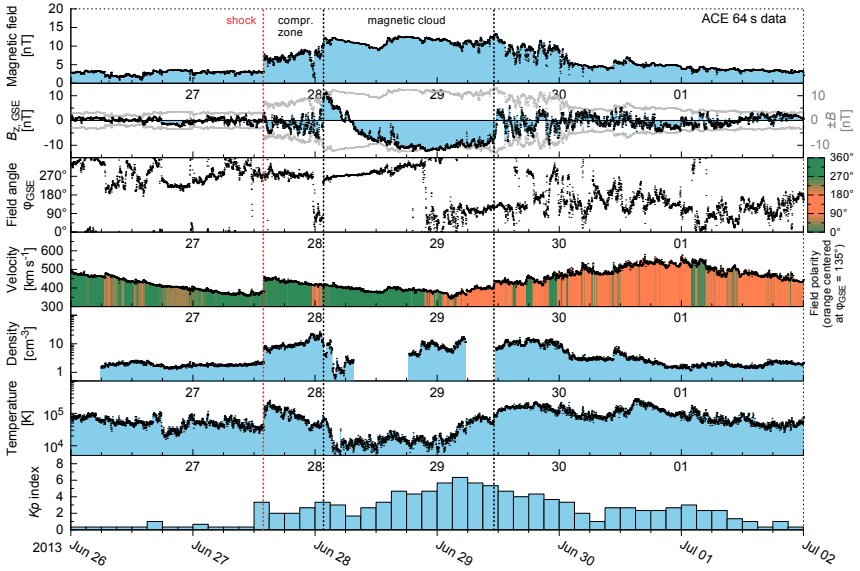
shock
compr. zone
magnetic cloud
ACE 64 s data
Magnetic field [nT]
$B_{z,GSE}$ [nT]
$\pm B$ [nT]
Field angle φ_{GSE}
Velocity [km s^{-1}]
Field polarity (orange centered at φ_{GSE} = 135°)
Density [cm^{-3}]
Temperature [K]
Kp index
2013 Jun 26
Jun 27
Jun 28
Jun 29
Jun 30
Jul 01
Jul 02

Solar wind and CME forecast

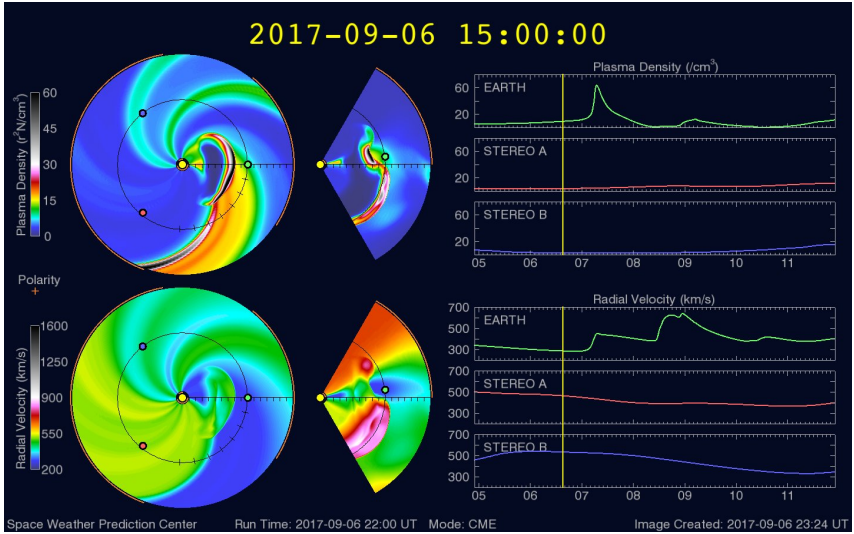

Credit: SWPC: WSA-Enlil Solar Wind Prediction. NOAA National Centers for Environmental Information

Kp long-term variations

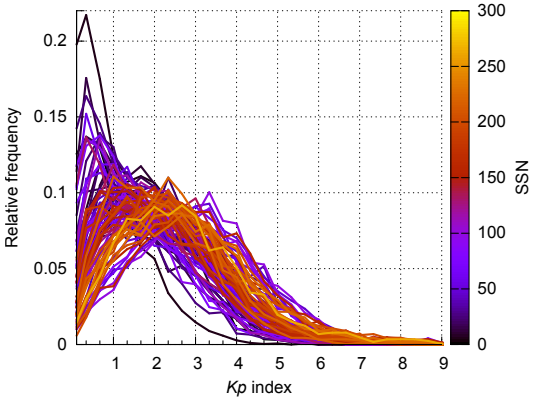

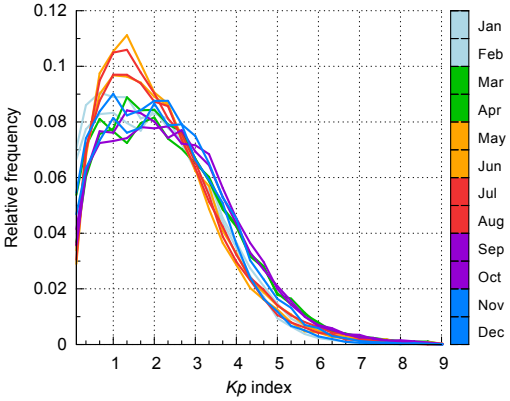

Prediction performance

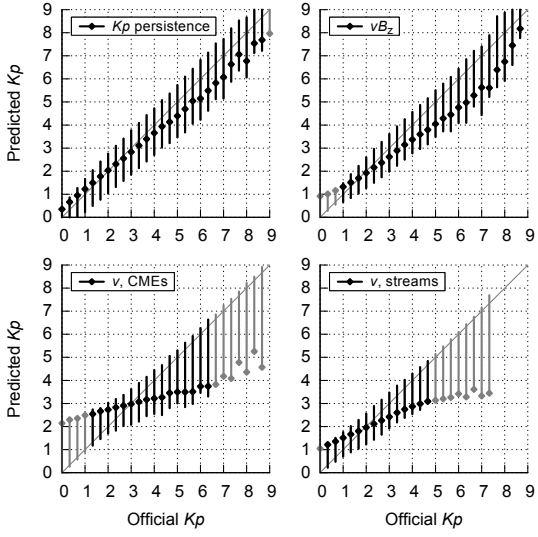

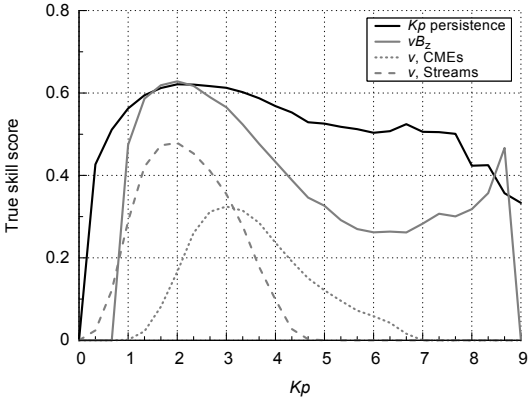

Empirical relations to predict the Kp index from solar wind electric field and from CME and stream velocity

Magnetosphere

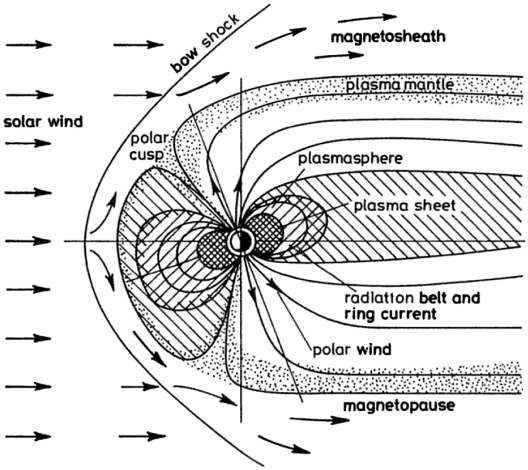

Credit: Davies (1990, Fig. 2.12)

4 interaction mechanisms

Magnetosphere

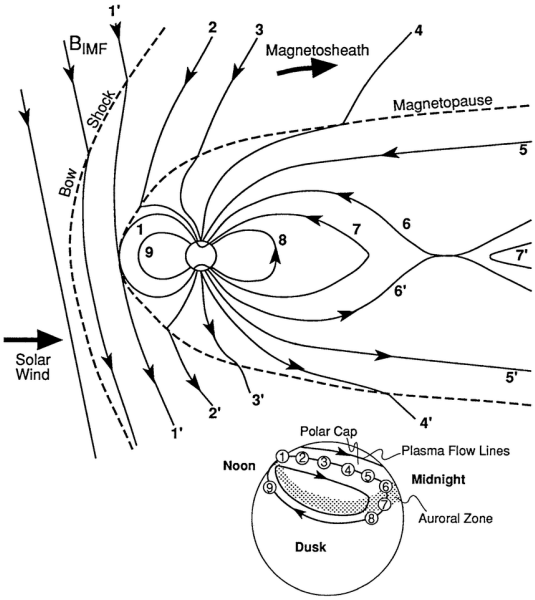

Credit: Hughes (1995, Fig. 9.11)

4 factors for merging flux rate

Kp index

13 observatories...

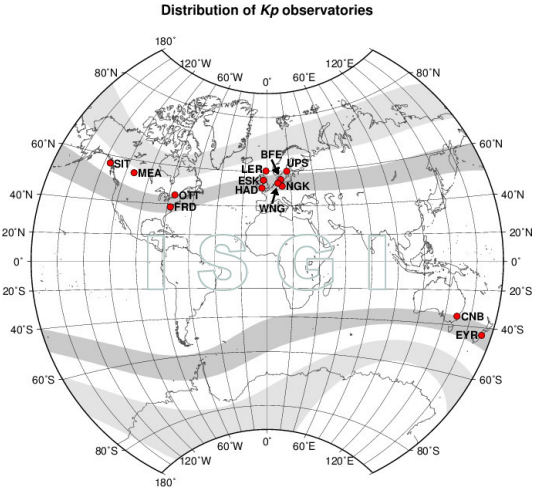

Courtesy of International Service of Geomagnetic Indices (ISGI), 2013

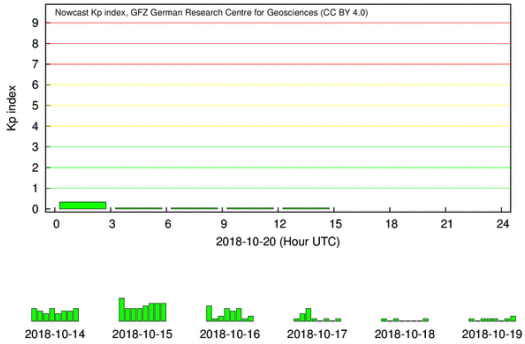

Credit: GFZ Potsdam, 2018

Solar wind electric field

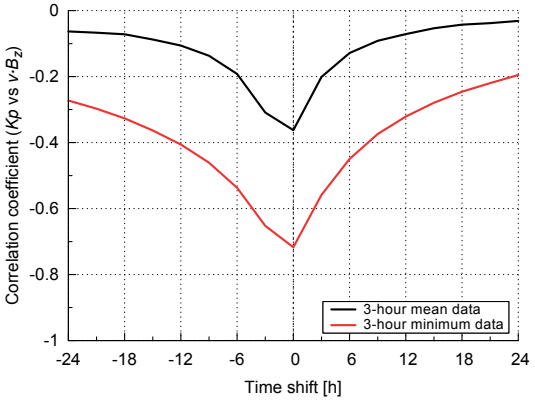

Solar wind electric field

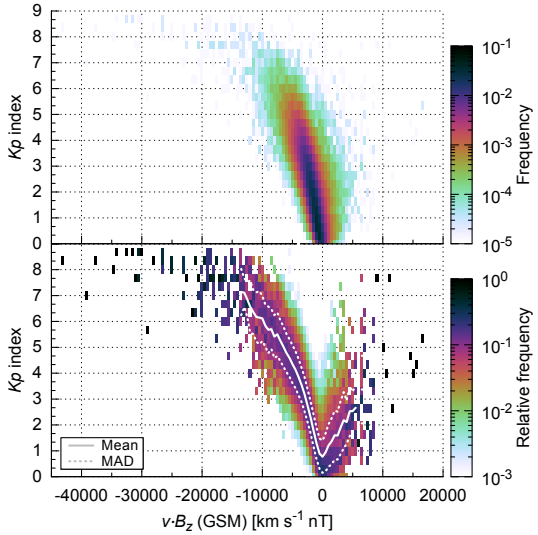

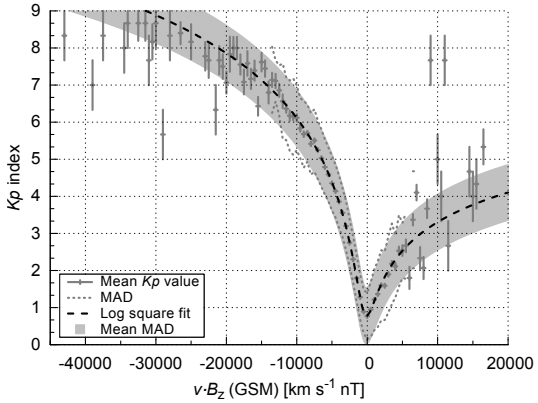

Solar wind velocity

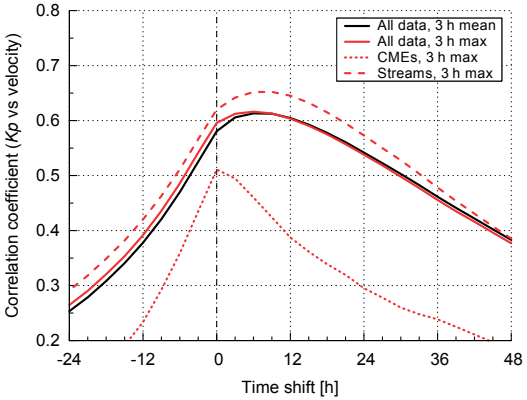

Solar wind velocity

CME – stream separation
Solar Wind Structures list

Solar wind velocity

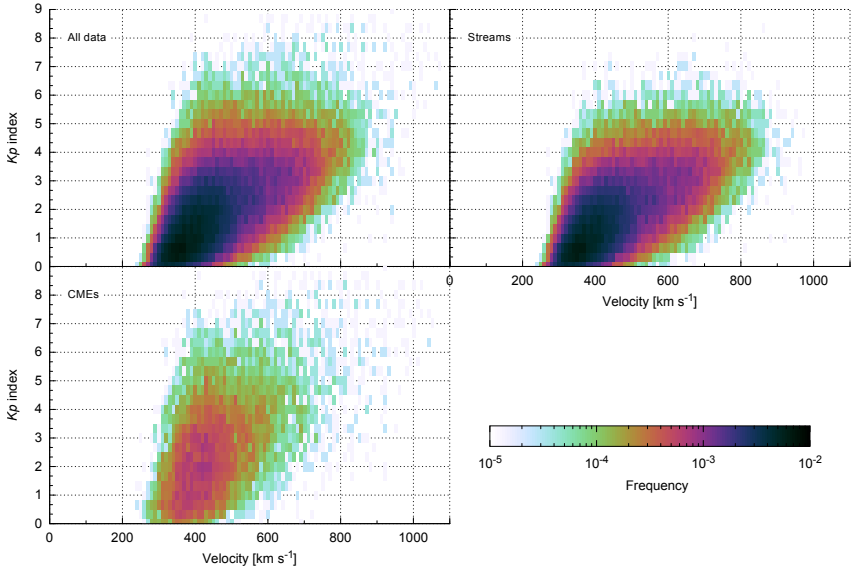

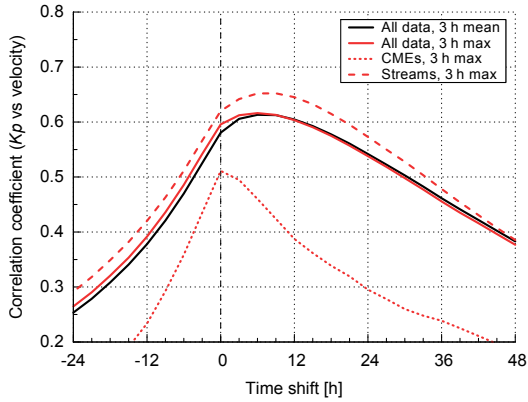
All data, 3 h mean
All data, 3 h max
CMEs, 3 h max
Streams, 3 h max
Correlation coefficient (Kp vs velocity)
Time shift [h]
0.8
0.7
0.6
0.5
0.4
0.3
0.2
-24
-12
0
12
24
36
48

CME velocity

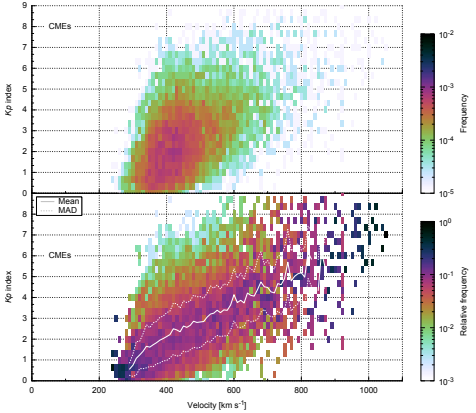

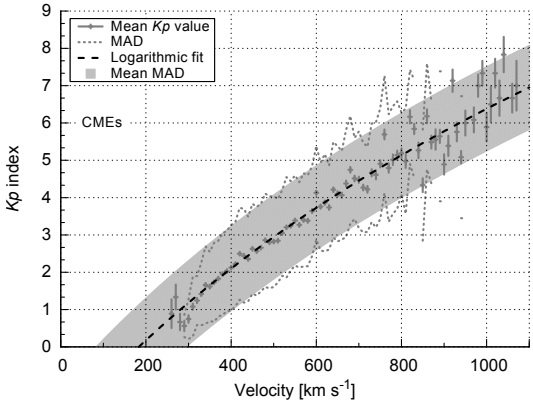

Stream velocity

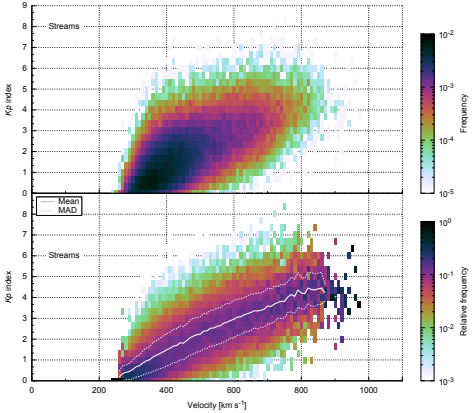

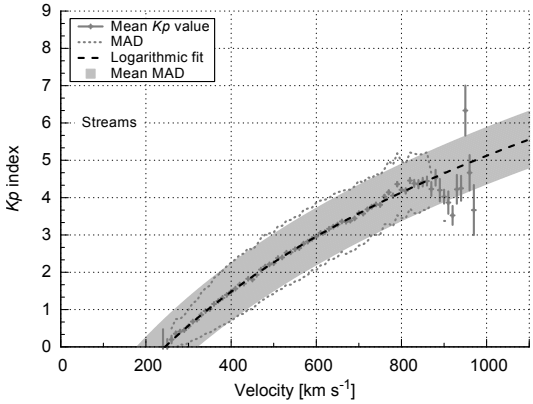

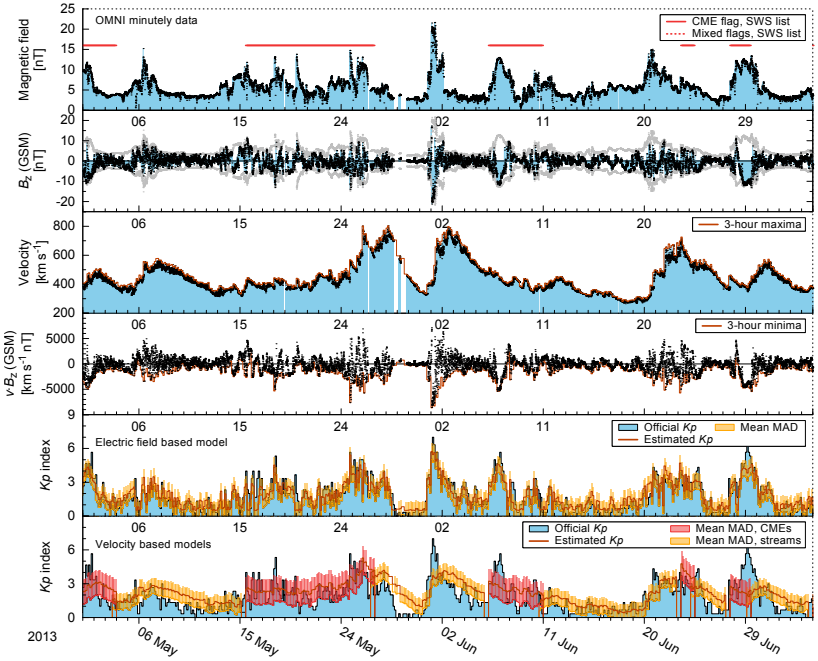
OMNI minutely data
CME flag, SWS list
Mixed flags, SWS list
Magnetic field [nT]
B_z (GSM) [nT]
σ_B [nT]
Velocity [km s^{-1}]
3-hour maxima
3-hour minima
$v \cdot B_z$ (GSM) [km s^{-1} nT]
Official Kp
Estimated Kp
Mean MAD
Electric field based model
Kp index
Mean MAD, CMEs
Mean MAD, streams
Velocity based models
2013
06 May
15 May
24 May
02 Jun
11 Jun
20 Jun
29 Jun

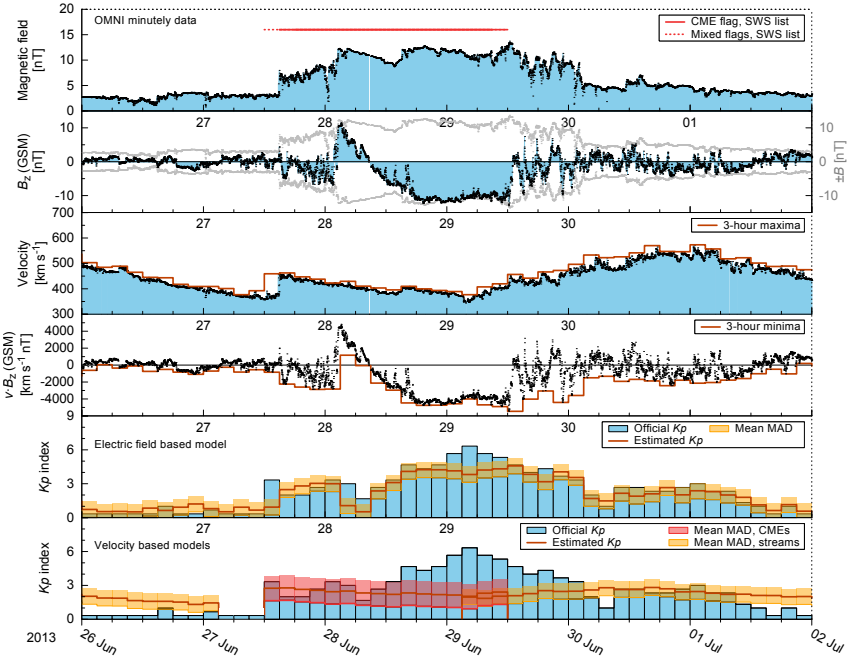
OMNI minutely data
CME flag, SWS list
Mixed flags, SWS list
Magnetic field [nT]
B_z (GSM) [nT]
±B [nT]
3-hour maxima
Velocity [km s^{-1}]
3-hour minima
$v \cdot B_z$ (GSM) [km s^{-1} nT]
Official Kp
Mean MAD
Estimated Kp
Electric field based model
Kp index
Mean MAD, CMEs
Mean MAD, streams
Velocity based models
2013
26 Jun
27 Jun
28 Jun
29 Jun
30 Jun
01 Jul
02 Jul

Results

Predictive Kp models based on relations with

- solar wind electric field proxy (vB_z)
- velocity of CME-associated flows (v_{CME})
- velocity of solar wind streams (v_{stream})

Conclusions

- The processing of 3-hour extrema of high time resolution data captures short-term geoeffective magnetic features that are neglected when averaging over 3-hour intervals
- The isolated treatment of CMEs and streams is beneficial to the prediction accuracy of Kp
- The prediction models perform well for their limited input information

⏩ Prediction performance

Lognormal distribution

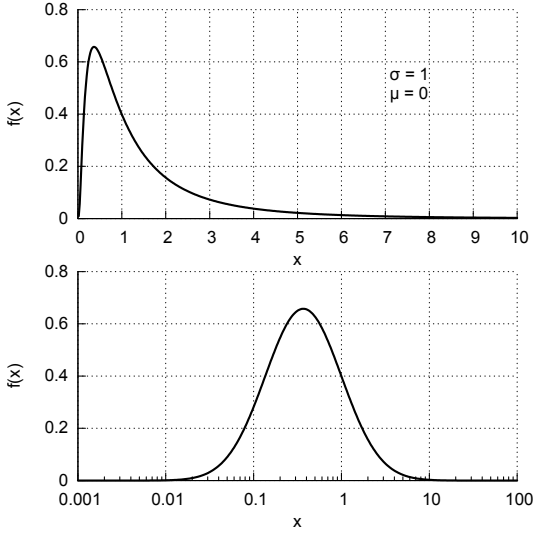

Probability density function:

$$f(x) = \frac{1}{\sigma\sqrt{2\pi}x}\, e^{-\frac{(\ln x-\mu)^2}{2\sigma^2}}$$

Location (μ) and shape parameter (σ).

Median and average:

$$x_{\text{med}} = \exp(\mu)\,, \qquad x_{\text{avg}} = \exp\left(\mu + \frac{\sigma^2}{2}\right)$$

$$f(x) = \frac{1}{2\sqrt{\pi \ln\left(\frac{x_{\text{avg}}}{x_{\text{med}}}\right)}\, x}\, \exp\left(-\frac{\ln^2\left(\frac{x}{x_{\text{med}}}\right)}{4\ln\left(\frac{x_{\text{avg}}}{x_{\text{med}}}\right)}\right)$$

Sun–Earth evolution of the solar wind

Solar wind measured in-situ throughout the heliosphere – except near-Sun

Sun–Earth evolution of the solar wind

special scientific interest:
coronal heating
solar wind acceleration

Solar activity

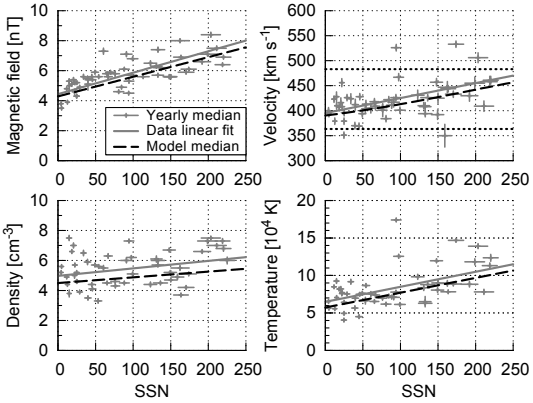

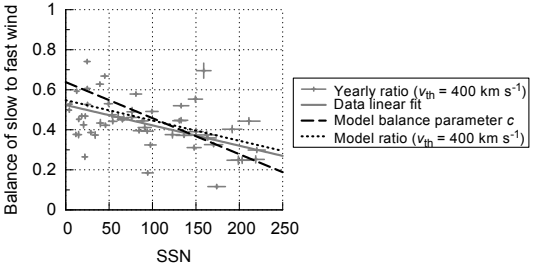

Solar wind model for the inner heliosphere and prediction of the near-Sun environment for the PSP orbit

combine models, extrapolation

PSP perihelia prediction